Supplement of Atmos. Chem. Phys., 25, 5087–5100, 2025
https://doi.org/10.5194/acp-25-5087-2025-supplement

Atmospheric Chemistry and Physics
Open Access
EGU

Supplement of

Hydrogen peroxide photoformation in particulate matter and its contribution to S(IV) oxidation during winter in Fairbanks, Alaska

Michael Oluwatoyin Sunday et al.

Correspondence to: Michael Oluwatoyin Sunday (mosunday@ucdavis.edu) and Cort Anastasio (canastasio@ucdavis.edu)

Table of contents

Table S1. Sample information and light absorption properties of particulate matter extracts

Sampling site	Sampling interval	Composite date [a]	No. of daily filters	Composite-Average Ambient PM2.5 ($\mu g\ m^{-3}$)	pH	PM-mass/H_2O mass [b] (10^{-4} µg-PM/µg-H_2O)	α_{300} (cm^{-1})	α_{365} (cm^{-1})	DOC (mg-C L^{-1})	MAC_{DOC} (300 nm) (m^2 $(g\text{-}C)^{-1}$)	MAC_{DOC} (365 nm) (m^2 $(g\text{-}C)^{-1}$)	AAE
House	1/13 - 1/17	1/15	4	7.5	0.90	2.8 (±1.8)	0.50	0.14	33.6	3.75	1.01	9.43
	1/17 - 1/25	1/21	8	12	1.2	2.6 (±1.4)	0.48	0.13	36.4	3.31	0.86	9.13
	1/26 - 1/28	1/27	2	17.7	4.4	3.0 (±0.6)	0.58	0.16	38.2	3.78	1.05	8.18
	1/29 - 2/3	1/31	5	26.1	1.3	3.2 (±0.1)	0.98	0.23	58.8	4.04	0.96	8.85
	2/3 - 2/6	2/4	3	8.6	1.1	1.7 (±0.3)	0.35	0.08	20.4	4.61	1.07	9.34
	2/6 - 2/8	2/7	2	4.3	0.88	4.7 (±0.1)	0.22	0.05	22.1	2.66	0.58	10.24
	2/8 - 2/21	2/14	13	7.2	1.2	1.9 (±0.6)	0.33	0.08	26.7	3.20	0.77	9.43
	2/21 - 2/23	2/22	2	3.6	1.1	1.8 (±0.2)	0.20	0.04	26.9	1.88	0.40	10.21
	2/23 - 2/26	2/24	3	12.5	1.2	3.3 (±0.4)	0.38	0.10	35.5	2.65	0.68	9.43
	Field Blank	n/a	1	n/a	1.3	1.2 (±0.2)	0.02	0.01	2.7	0.25	0	n/a
CTC	1/17 - 1/25	1/21 pH 1	8	12.0	1.3	2.1 (±0.1)	0.46	0.13	32.4	3.56	1.01	8.24
		1/21 pH 3[c]			3.1	n.d.	n.d.	n.d.	n.d.	n.d.	n.d.	n.d.
		1/21 pH 5 [c]			5.0	n.d.	0.48	0.15	32.4	3.72	1.16	7.3
	2/6 - 2/8	2/7	2	4.3	1.2	1.8 (±0.1)	0.22	0.05	22.4	2.06	0.52	9.13
	2/8 - 2/21	2/14	13	This sample was used for the dilution series experiments. See Tables S5a – S5c for sample data.								
	2/21 - 2/23	2/22 pH 1 [c]	2	3.6	1.0	n.d	n.d	n.d	n.d	n.d	n.d	n.d
		2/22 pH 5			5.0	2.2 (±0.4)	0.22	0.06	21.2	2.39	0.65	7.65

[a] The composite date represents the day at the midpoint of sampling interval. For composites with an even number of sampling days, the midpoint date is determined based on the total number of sampling hours. All samples were collected in 2022. Date format is month/day.

[b] The PM-mass/H_2O mass ratio was determined by dividing the PM mass extracted (i.e., the difference in filter mass before and after extraction) from each 2 cm x 2 cm square filter by the volume of solvent (1.0 mL) used for the extraction. Three to five squares are usually extracted from each filter in a composite and the total mass extracted is divided by the total volume of solvent.

[c] For results labelled n.d. (not determined), the samples (CTC 1/21 pH 3 and CTC 2/22 pH 1) were not characterized because of a limited amount of filter.

Table S2. Concentration of ions (in µM) in extracts of PM samples

Sampling site	Composite date	Cl^-	NO_2^-	Br^-	NO_3^-	SO_4^{2-}	PO_4^{3-}	Na^+	NH_4^+	K^+	Mg^{2+}	Ca^{2+}
House	1/15	40	0	2	272	381	19	201	612	38	10	23
	1/21	72	0	3	268	430	23	507	1391	84	35	60
	1/27	69	0	0	437	569	19	717	1719	69	49	58
	1/31	53	0	4	291	585	20	194	828	57	9	27
	2/4	34	0	5	170	318	16	454	1043	43	28	39
	2/7	48	0	4	84	187	19	220	291	21	9	26
	2/14	49	0	1	163	356	32	526	1102	47	39	82
	2/22	9	0	6	145	241	25	375	836	24	18	69
	2/24	37	1	0	276	307	27	181	560	39	5	42
	Field Blank	6	0	0	9	2	15	286	0	10	5	4
CTC	1/21	169	7	8	556	1058	21	662	2442	116	69	126
	2/7	50	0	4	154	289	15	262	412	28	8	24
	2/14	This sample was used for the dilution series experiments. See Tables S5c for ion data.										
	2/22	241	6	4	438	544	0	1618	1121	107	63	133

[a] Ions were measured in a separate sample prepared by extracting the filter square with Milli-Q with no pH adjustment. The solvent-to-filter ratio was the same as the standard extract: 1.0 mL Milli-Q for a 2 cm × 2 cm square of filter.

Table S3. Photoformation rates, loss rate constants, rates of light absorption and quantum yields of HOOH in PM extracts under laboratory illumination.

Sampling site	Composite date	pH	$j_{2NB,EXP}$ [a] (s^{-1})	$P_{HOOH,PME,EXP}$ [b] ($\mu M\ h^{-1}$)	$k_{HOOH,PME,EXP}$ [c] (h^{-1})	$R_{abs,PME,EXP}$ [d] (10^{-5} mol photons $L^{-1}\ s^{-1}$)	$R_{abs,PME,AK}$ [e] (10^{-5} mol photons $L^{-1}\ s^{-1}$)	$R_{abs,PME,AK}$ / $R_{abs,PME,EXP}$ [f]	$10^2 \times \Phi_{HOOH}$
House site	1/15	0.90	0.021	110 (±21)	2.8 (±1.0)	3.5	0.49	0.14	0.09 (±0.02)
	1/21	1.2	0.022	133 (±8)	4.8 (±0.4)	3.5	0.33	0.09	0.11 (±0.01)
	1/27	4.4	0.022	57 (±0.1)	4.1 (±0.5)	5.1	0.66	0.13	0.03 (±0.01)
	1/31	1.3	0.021	344 (±22)	6.5 (±0.6)	6.9	1.40	0.20	0.14 (±0.01)
	2/4	1.1	0.021	79 (±4)	4.1 (±0.4)	2.3	0.33	0.14	0.09 (±0.01)
	2/7	0.88	0.022	66 (±5)	4.3 (±0.5)	1.3	0.26	0.20	0.14 (±0.01)
	2/14	1.2	0.022	91 (±5)	1.2 (±0.2)	2.2	0.62	0.28	0.12 (±0.01)
	2/22	1.1	0.022	40 (±6)	3.7 (±1.0)	1.1	0.21	0.19	0.10 (±0.02)
	2/24	1.2	0.022	77 (±12)	3.2 (±0.8)	2.6	1.00	0.38	0.08 (±0.01)
	Field Blank[g]	1.3	0.020	2 (±0.15)	3.0 (±0.3)	-	-	-	-
CTC site	1/21	1.3	0.015	122 (±10)	3.5 (±0.4)	4.1	0.38	0.09	0.08 (±0.01)
		3.1	0.017	81 (±10)	3.3 (±0.5)	n.d.	n.d.	-	0.06 (±0.01)
		5.0	0.015	45 (±5.6)	1.7 (±0.3)	5.0	0.46	0.09	0.03 (±0.00)
	2/7	1.2	0.020	33 (±1.4)	1.6 (±0.1)	1.5	0.28	0.19	0.06 (±0.00)
	2/14 [h]	~ 1	0.020	29 (±1)	3.1 (±0.2)	3.0	0.84	0.28	0.03(±0.00)
	2/22	1.0	0.017	38 (±4.9)	4.6 (±0.7)	n.d.	n.d.	-	0.05 (±0.01)
		5.0	0.015	4.6 (±0.9)	1.0 (±0.3)	2.2	0.38	0.17	-

[a] Rate constant for the direct photochemical loss of 2-nitrobenzaldehyde, our chemical actinometer, on the day of each experiment.

[b] Photoformation rate of HOOH in a PM extract during illumination with laboratory simulated sunlight. Values in parentheses are 1 standard error obtained from the kinetic fits of the experimental data (equation 3). So that rates can be better compared, they have all been normalized to a j_{2NB} value of 0.020 s^{-1}:

$$P_{HOOH,PME,EXP} = P^*_{HOOH,PME,EXP} \times \left(\frac{0.020}{j_{2NB,EXP}}\right)$$

where $P^*_{HOOH,PME,EXP}$ is the unnormalized HOOH formation rate measured from the experiment and $P_{HOOH,PME,EXP}$ is the HOOH formation rate normalized to a 2NB photolysis rate constant of 0.020 s^{-1}.

[c] Rate constant for loss of HOOH during simulated sunlight illumination, with errors of 1 standard error obtained from the kinetic fit of the experimental data (equation 3).

[d] Rate of light absorption by the extract during simulated sunlight illumination in the lab, calculated from 300 to 550 nm. Values have been normalized to a photon flux corresponding to a j_{2NB} value of 0.020 s^{-1}.

[e] Rate of sunlight absorption by the extracts using actinic fluxes measured in Fairbanks, Alaska, calculated from 310 to 550 nm; see equation 2. The actinic flux used is the 3-hr average midday value for each day, averaged for all the days in the composite.

[f] Ratio of rate of absorption of light by the extract under Fairbanks, Alaska actinic flux compared to the rate of light absorption under illumination by the solar simulator.

[g] The field blank is a blank filter that was placed in the Hi-Vol Air sampler for a few minutes without air flow. The filter was then shipped, stored, and later extracted following the same procedure as the filters used for particle collection.

[h] Data for this sample at a concentration factor of 1 (corresponding to 1.0 mL of H_2SO_4 solution used to extract each filter square) was extrapolated from the dilution series data in Table S5

Table S4a. Concentrations of dissolved metals (in µM) in pH 1 extracts

Sampling site	Composite date	Fe	Cu	Mn	V	Ni
House	1/15	6.52	0.94	0.32	0.02	0.07
	1/21	8.85	0.71	0.32	0.01	0.07
	1/27, pH 4 [a]	n.d.	n.d.	n.d.	n.d.	n.d.
	1/31	11.04	1.24	0.37	0.02	0.06
	2/4	6.19	0.49	0.20	0.02	0.11
	2/7	2.42	0.26	0.11	0.01	0.09
	2/14	5.17	0.58	0.17	0.02	0.02
	2/22	2.94	0.29	0.10	0.01	0.16
	2/24	10.08	0.95	0.28	0.01	0.08
	Blank	1.13	0.03	0.01	0.01	0.04
CTC	1/21, pH 1	9.53	0.89	0.47	0.02	0.07
	1/21, pH 3	5.64	0.83	0.42	0.01	0.12
	1/21, pH 5	2.19	0.52	0.30	0.01	0.04
	2/7	3.56	0.40	0.17	0.02	0.06
	2/14	This sample was used for the dilution series experiments. See Table S5b for metals data.				
	2/22, pH 1	6.29	14.78[b]	0.82	0.02	0.63
	2/22, pH 5	0.64	9.42[b]	0.52	0.01	0.36

[a] This sample was not analyzed for metals due to a shortage of filter for this composite.

[b] These copper concentrations are unreasonably high, indicating that these sample aliquots used for metal analysis are contaminated with copper (and perhaps other metals). However, the remainder of this composite extract appears to be unaffected by contamination, based on the measured rate constants for HOOH loss during illumination. Measured values of $k_{HOOH,PME,EXP}$ are 4.6 (± 0.7) and 1.0 (± 0.3) hr^{-1}, at pH 1 and 5, respectively, which are within the range of the other samples (Table S3). In contrast, calculated k_{HOOH} values for the 2/22 CTC samples based on the Cu concentrations in this table are 19 and 11 hr^{-1} for the pH 1 and 5 extracts, respectively, which are much higher than measured rate constants. This suggests that the illuminated extracts were unaffected by copper contamination,

Table S4b. Concentrations of dissolved metals (in µM) in Milli-Q extracts of House samples

Sampling site	Composite date	Fe	Cu	Mn	V	Ni
House	1/15	1.34	0.44	0.23	0.01	0.05
	1/21	1.22	0.38	0.21	0.01	0.04
	1/27 [a]	n.d.	n.d.	n.d.	n.d.	n.d.
	1/31	2.96	0.70	0.29	0.01	0.05
	2/4	0.67	0.22	0.13	0.01	0.06
	2/7	0.08	0.05	0.07	0.01	0.02
	2/14	0.20	0.17	0.11	0.01	0.01
	2/22	0.05	0.05	0.05	0.01	0.01
	2/24	0.28	0.22	0.17	0.01	0.01
	Blank	0.01	0.01	0.00	0.00	0.01
CTC[b]	2/7	0.55	0.17	0.10	0.01	0.03

[a] This sample was not analyzed for metals due to a shortage of filters for this composite.

[b] This is the only CTC composite sample that was analysed for metals in the MQ extract.

Table S5a. Characteristics of the dilution series performed on the CTC 2/14 composite (pH 1)

Concentration factor (CF) [a]	PM mass/H_2O mass (10^{-4} µg-PM/µg-H_2O)	α_{300} (cm^{-1})	α_{365} (cm^{-1})	[DOC] (mg-C L^{-1})	$P_{HOOH,PME,EXP}$ (µM h^{-1})	$k_{HOOH,PME,EXP}$ (h^{-1})	$R_{abs,PME,EXP}$ [b] (10^{-5} mol photons L^{-1} s^{-1})	$10^2 \times \Phi_{HOOH}$ (%)
0.10	0.18 [c]	0.04	0.01	2.72	2.7 (±0.12)	1.20 (±0.20)	0.3	0.020 (±0.001)
0.50	0.89 [c]	0.19	0.05	13.8	22 (±2.4)	3.00 (±0.50)	1.4	0.025 (±0.004)
1.43	2.55	0.57	0.16	35.6	40 (±4.2)	4.80 (±0.20)	4.2	0.024 (±0.003)
2.50	4.5 [c]	0.89	0.28	61.7	71 (±3.2)	7.70 (±1.00)	8.8	0.020 (±0.001)
3.33	6.0 [c]	1.1	0.34	78.7	98 (±18)	12.00 (±1.31)	9.8	0.026 (±0.006)
R^2 [d]		0.996	0.994	0.999	0.991	0.990	0.980	0.002
p-value		< 0.01	< 0.01	< 0.01	< 0.01	< 0.01	< 0.01	> 0.05

[a] The Concentration Factor is the inverse of the volume of solvent (10., 2.0, 0.70, 0.40 or 0.30 mL) used to extract a given dilution.
[b] $R_{abs,PME,EXP}$ is the rate of absorption of light by the extract in the solar simulator.
[c] Because of limited filter amount, these values were estimated from a linear regression of this parameter versus concentration factor from the 1.43 CF sample.
[d] Correlation coefficient for the relationship between a given parameter and concentration factor. See Figure S4 for plots of some of the relationships.

Table S5b. Metals content (µM) of the CTC 2/14 dilution series extracts (pH 1)

Concentration factor (CF)	Fe	Cu	Mn	V	Ni
0.10	1.23	0.95	0.04	0.03	0.01
0.50	5.32	4.69	0.17	0.10	0.04
1.43	13.27	13.70	0.43	0.05	0.08
2.50	21.34	21.47	0.83	0.08	0.22
3.33	26.59	31.10	0.97	0.20	0.20
R^2	0.995	0.995	0.996	0.59	0.905
p-value	< 0.01	< 0.01	< 0.01	> 0.05	< 0.05

Table S5c. Concentrations of ions (μM) in the CTC 2/14 dilution series Milli-Q extracts

Concentration factor (CF)[a]	Na^+	NH_4^+	K^+	Mg^{2+}	Ca^{2+}	Cl^-	NO_2^-	Br^-	NO_3^-	SO_4^{2-}	PO_4^{3-}
0.10	105	113	11	0	0	16	0	0	27	49	0
0.50	244	427	42	4	17	55	0	0	157	260	10
1.43	495	856	105	13	46	141	0	0	433	701	17
R^2	0.996	0.981	0.999	0.999	0.995	0.999	n/a	n/a	0.999	0.999	0.887
p-value	<0.05	>0.05	<0.05	<0.05	<0.05	<0.01	n/a	n/a	<0.05	<0.05	>0.05

[a] Because of a limited amount of filter, we did not make Milli-Q extracts for the two most concentrated extract conditions and thus did not analyze ions for these dilutions.

Table S6. Aerosol liquid water content (ALWC), DOC, concentration of inorganic S(IV), HOOH formation rate and loss rate constant in ambient particles under ALW conditions

Sampling site	Composite date	ALWC ($\mu g\ m^{-3}$)[a]	Ionic strength (M)	$[DOC]_{ALW}/[DOC]_{PME}$ [a]	$P_{HOOH,ALW,AK}$ ($M\ h^{-1}$) [b]	$k_{HOOH,ALW,AK}$ (h^{-1}) [c]	Inorganic S(IV) (mM) [d]	$k_{HOOH,ALW,AK}$ due to S(IV) (h^{-1})[e]
House	1/15	9.4	n.d.	6161	0.09	2×10^{4}	n.d.	n.d.
	1/21	12.1	13.0	6024	0.08	3×10^{4}	40	4×10^{8}
	1/27	11.2	14.2	6445	0.05	3×10^{4}	20	1×10^{8}
	1/31	16.0	15.1	4516	0.3	3×10^{4}	70	1×10^{9}
	2/4	4.9	22.9	14634	0.2	6×10^{4}	4	4×10^{7}
	2/7	1.9	17.9	38563	0.5	2×10^{5}	6	4×10^{7}
	2/14	6.1	13.6	11817	0.3	1×10^{4}	20	4×10^{8}
	2/22	9.5	5.3	7569	0.06	3×10^{4}	2	2×10^{7}
	2/24	31.9	5.2	2264	0.07	7×10^{3}	90	5×10^{8}
CTC	1/21	12.1	13.0	3734	0.04	1×10^{4}	n.d.	n.d.
	2/7	1.9	17.9	27148	0.2	4×10^{4}		
	2/14	6.1	13.6	8272	0.07	3×10^{4}		
	2/22	9.5	5.3	5440	0.04	7×10^{3}		

[a] Values for ALWC, ionic strength, and $[DOC]_{ALW}/[DOC]_{PME}$ are from (Heinlein et al., 2025).

[b] $P_{HOOH,ALW,AK}$ was determined as described in section 3.4 (equation 5) of the main text.

[c] $k_{HOOH,ALW,AK}$ was determined as described in section 3.4 of the main text using an equation analogous to equation 5. These values are based on measured rate constants for HOOH loss in the particle extracts; they do not include any contribution from inorganic S(IV).

[d] Modeled concentrations of inorganic S(IV) in particle water are from Heinlein et al. (2025).

[e] "$k_{HOOH,ALW,AK}$ due to S(IV)" is the rate constant for loss of HOOH due to reaction with inorganic S(IV) in the particles.

Section S1. Loss rate constant of S(IV)

The pseudo-first-order rate constant (s^{-1}) for loss of S(IV) due to reaction with HOOH in the particles was calculated according to equations S1- S2 (McArdle and Hoffmann, 1983):

$$k_{HOOH,ALW,S(IV)} = k4[H^+][HSO3^-]/(1+K[H^+]) \text{ ,} \quad \text{(S1)}$$

$$\text{where } k_4 = 7.45x10^7 e^{-4430\,(\frac{1}{T}-\frac{1}{298})} \quad \text{(S2)}$$

and K = 13 M^{-1}. k_4 was adjusted for the effect of ionic strength using equation S3 (Maaß et al., 1999):

$$log_{10}\left(\frac{k_4^{ALW}}{k_4^0}\right) = 0.36I_s - \frac{1.018\sqrt{I_s}}{1+0.17\sqrt{I_s}} \text{ ,} \quad \text{(S3)}$$

where k_4 is the third-order apparent reaction rate constant (M^{-2} s^{-1}) of HSO_3^- with HOOH in dilute solution with an ionic strength (I_s) close to 0, k_4^{ALW} is the rate constant at high I_s, typical of deliquesced aerosols, and K is the equilibrium constant (M^{-1}). The concentration of inorganic S(IV) is presented in Table S18 of (Heinlein et al., 2025). Liu et al. (2020) report that the oxidation of SO_2 by HOOH in deliquesced aerosol is enhanced at the high ionic strength typical of aerosol liquid water (ALW) conditions. However, since S(IV) is already the dominant sink for HOOH in ALW with the equations above (see section 3.5 in the main text), we did not include the enhancement observed by Liu et al. since it would have no impact on the production rate of sulfate, which is equal to the rate of formation of HOOH.

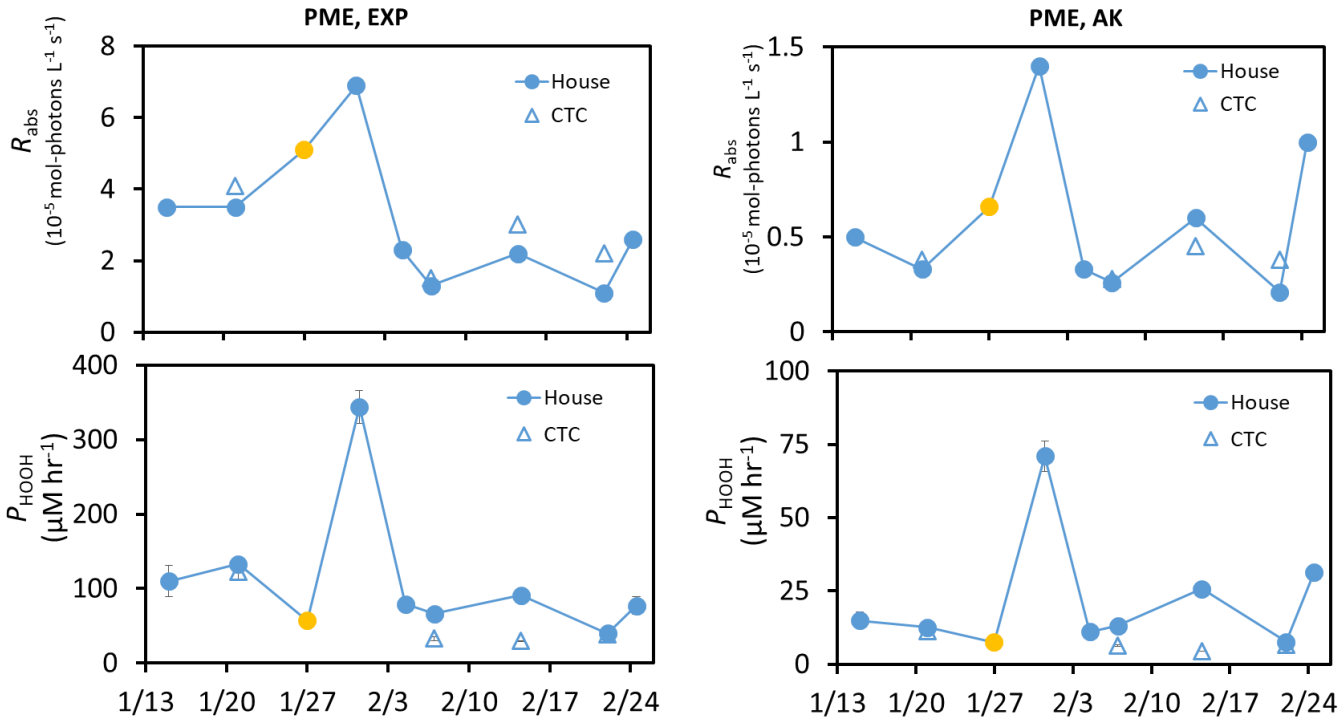

Figure S1. Comparison of rates of light absorption (top row) and HOOH photoformation (bottom row) for two light conditions: (1) laboratory simulated sunlight, normalized to a constant photon flux of $j_{2NB} = 0.020\ s^{-1}$ (left column), and (2) the average of the measured midday Fairbanks actinic fluxes (downwelling and upwelling) for the days of each composite, including an enhancement factor of 2.5 for optical confinement within particles. The left two panels are the same as shown in panels A and B in Figure 2 of the main text. Filled circles represent data for PM collected from the House site, while open triangles are for CTC samples. Blue symbols are pH 1 extracts, while gold symbols are pH 4 or 5. Note the difference in the y-axis scales between the two columns.

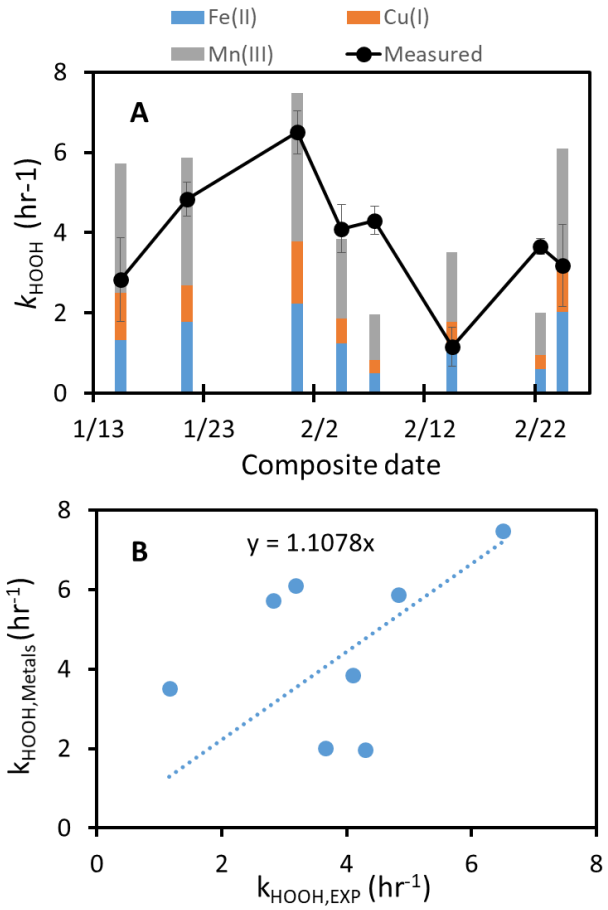

Figure S2. Rate constants for the loss of HOOH in the House samples, both experimentally determined ($k_{HOOH,PME,EXP}$) and calculated ($k_{HOOH,Metals}$) in the based on reactions with dissolved Fe, Cu, and Mn in each extract. We calculated values of $k_{HOOH,calc}$ using: (1) measured dissolved Fe, Cu, and Mn concentrations in each extract (Table S4), (2) assuming 80%, 5%, and 100% of the dissolved iron, copper, and manganese were present as Fe(II), Cu(I), and Mn(III), respectively (Deguillaume et al., 2005; Siefert et al., 1998), and (3) reaction rate constants of 70 M^{-1} s^{-1} for HOOH + Fe(II), 7000 M^{-1} s^{-1} for HOOH + Cu(I) and 2800 M^{-1} s^{-1} for HOOH + Mn(III) (Song et al., 2021). The Mn contribution to HOOH loss here is an upper bound, assuming that all dissolved manganese is present as Mn(III), which is an overestimate. If we assume that all Mn is present as Mn(II), the manganese contribution to HOOH loss is negligible (see Figure 3A in main text).

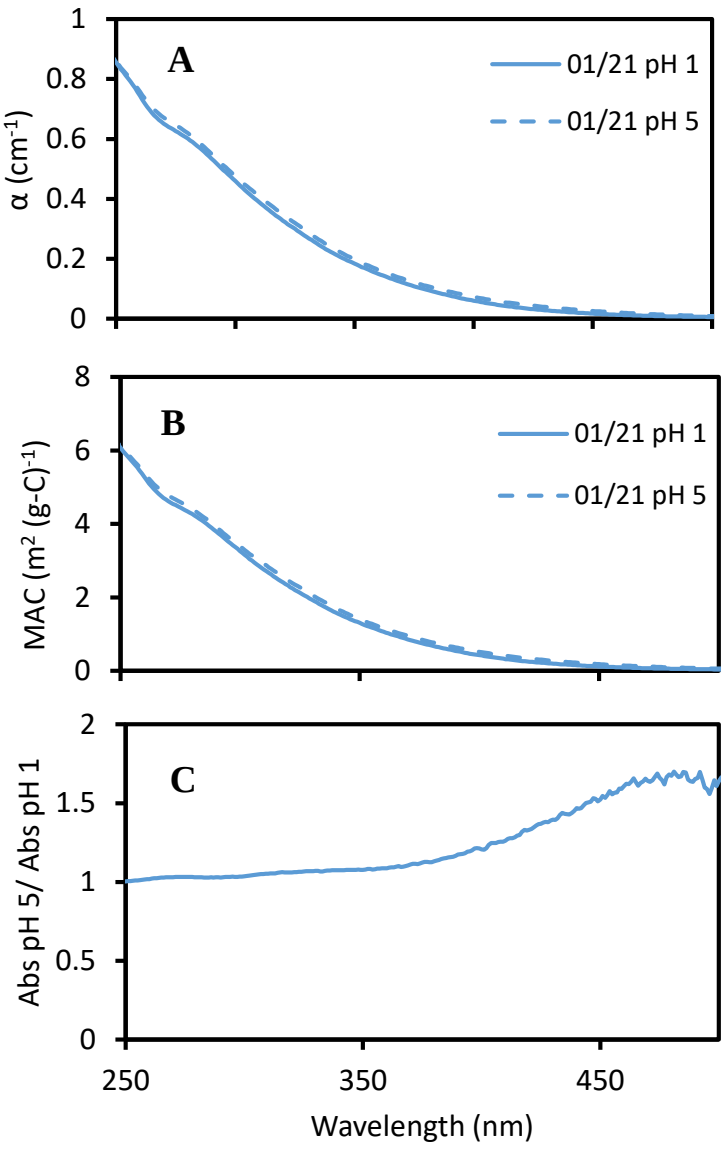

Figure S3. pH dependence of light absorption for a PM extract. (A) UV-visible spectra of the 1/21 composite from the CTC site at pH 1 and 5. (B) the corresponding DOC-normalized mass absorption coefficients. Panel (C) shows the ratio of the pH 5 and pH 1 absorbance values for the sample.

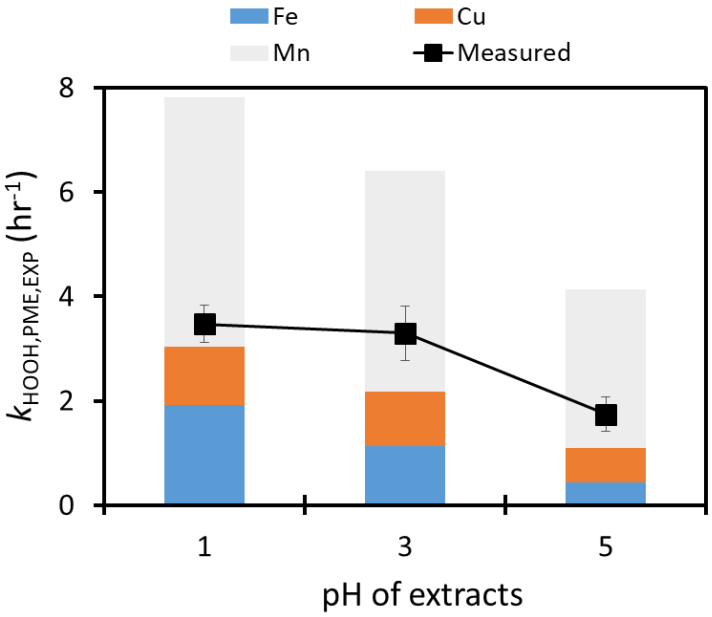

Figure S4. Rate constants for the loss of HOOH as a function of pH in extracts from the CTC particles of 1/21. The experimentally determined loss rate constants (EXP) are represented by black squares while the calculated loss rate constants due to HOOH reaction with Fe, Cu, and Mn are shown by the stacked bars. As described in the text, the value of k_{HOOH} due to Mn(II) is negligible; the Mn bars shown here are an upper bound, assuming that all the dissolved Mn (Table S4) is present as Mn(III) during illumination.

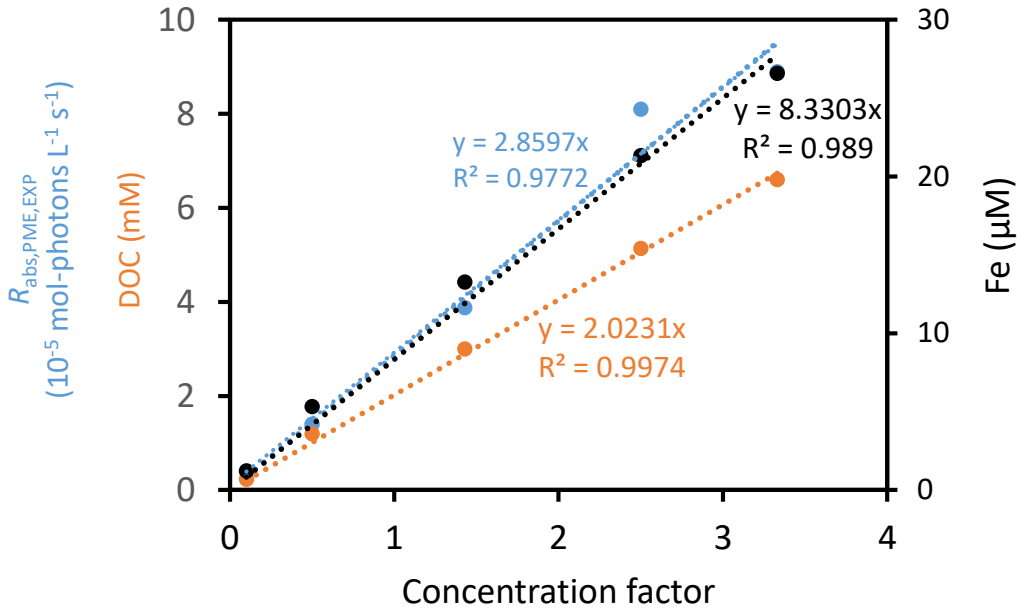

Figure S5. Rate of light absorption, DOC content and Fe content of the extracts used in the dilution series experiment using CTC composite 2/14 at pH 1. The concentration factor (CF), a measure of the concentration of an extract (with 0 being an infinite dilution), is equal to the inverse of the volume of solvent used per filter square.

References

Deguillaume, L., Leriche, M., Desboeufs, K., Mailhot, G., George, C., and Chaumerliac, N.: Transition Metals in Atmospheric Liquid Phases: Sources, Reactivity, and Sensitive Parameters, Chem. Rev., 105, 3388–3431, https://doi.org/10.1021/cr040649c, 2005.

Heinlein, L. M. D., He, J., Sunday, M. O., Guo, F., Campbell, J., Moon, A., Kapur, S., Fang, T., Edwards, K., Cesler-Maloney, M., Burns, A., Dibb, J., Simpson, W., Shiraiwa, M., Alexander, B., Mao, J., Flynn, J. H., Stutz, J., and Anastasio, C.: Unexpectedly Robust Photochemistry in Subarctic Particles During Winter: Evidence from Photooxidants, https://egusphere.copernicus.org/preprints/2025/egusphere-2025-824/, 2025.

Liu, T., Clegg, S. L., and Abbatt, J. P. D.: Fast oxidation of sulfur dioxide by hydrogen peroxide in deliquesced aerosol particles, Proceedings of the National Academy of Sciences, 117, 1354–1359, https://doi.org/10.1073/pnas.1916401117, 2020.

Maaß, F., Elias, H., and Wannowius, K. J.: Kinetics of the oxidation of hydrogen sulfite by hydrogen peroxide in aqueous solution:, Atmospheric Environment, 33, 4413–4419, https://doi.org/10.1016/S1352-2310(99)00212-5, 1999.

McArdle, J. V. and Hoffmann, M. R.: Kinetics and mechanism of the oxidation of aquated sulfur dioxide by hydrogen peroxide at low pH, J. Phys. Chem., 87, 5425–5429, https://doi.org/10.1021/j150644a024, 1983.

Siefert, R. L., Johansen, A. M., Hoffmann, M. R., and Pehkonen, S. O.: Measurements of Trace Metal (Fe, Cu, Mn, Cr) Oxidation States in Fog and Stratus Clouds, Journal of the Air & Waste Management Association, 48, 128–143, https://doi.org/10.1080/10473289.1998.10463659, 1998.

Song, H., Lu, K., Ye, C., Dong, H., Li, S., Chen, S., Wu, Z., Zheng, M., Zeng, L., Hu, M., and Zhang, Y.: A comprehensive observation-based multiphase chemical model analysis of sulfur dioxide oxidations in both summer and winter, Atmos. Chem. Phys., 21, 13713–13727, https://doi.org/10.5194/acp-21-13713-2021, 2021.